AIAA-2008-3745

38th AIAA Fluid Dynamics Conference and Exhibit, June 23-26 2008, Seattle, WA

Turbulent Drag Reduction using Sinusoidal Riblets with Triangular Cross-Section

Yulia Peet* and Pierre Sagaut†

Université Pierre et Marie Curie - Paris 6, 75252 Paris, France

Yves Charron‡

IFP- Institut Français du Pétrole, 92852 Rueil Malmaison, France

It is known that longitudinal ribs manufactured in a flat surface act to reduce turbulent skin-friction drag, providing a moderate drag reduction of 4 to 8%. It is shown in this paper that this value can be increased by at least 50% if sinusoidal-like rods are used instead of conventional straight riblets. Large Eddy Simulation of a turbulent flow over a riblet-covered surface is performed for three cases: straight riblets and sinusoidal riblets with two different values of wavelength. All riblets have triangular cross-section. It is found that drag reduction with sinusoidal riblets depend strongly on the wavelength, showing a benefit over straight riblets for a larger value of the wavelength, and an opposite trend - for a smaller value. Different nature of the flow over straight and sinusoidal riblet surfaces is revealed by looking at crossflow motion in transverse planes, mean and instantaneous streamwise vorticity, and organized coherent structures. Turbulent statistics is compared between all three cases, crossflow turbulence intensity is reduced for sinusoidal riblets as opposed to straight riblets.

I. Introduction

Riblets, or wall grooves manufactured in a surface, are attractive drag-reducing devices because of their low production cost and easiness of maintenance.[1–8] They can be successfully installed on wings of an aircraft, hull of a submarine or internal walls of a gas pipeline by adding special plastic films with sub-millimeter scale riblets which are available commercially.[7,9] An unfortunate disadvantage of riblets is rather low amount of drag reduction which they can offer: the best values have been achieved with infinitely-thin blade riblets giving about 10% reduction for an optimized configuration;[8] while more realistic cross-sections for industrial use, such as triangular, V-groove or scalloped, usually account for 4–8% drag reduction.[1–8] An easy modification to the riblet method, retaining its structural simplicity but improving its drag reduction performance, would be more than welcome!

One of the new methods proposed in literature devoted to turbulent skin-friction drag reduction is high-frequency spanwise wall oscillations.[10–15] It is argued that oscillatory motion of the wall makes longitudinal boundary layer vortices move in a sinuous form, which reduces their strength and, consequently, their ability to produce turbulence through near-wall burst events,[16] resulting in a lower turbulent skin-friction drag. In practical applications, it is usually not possible to provide sustainable oscillations of the surface. However, if one can mimic such an oscillatory motion with the help of some passive devices, that should have more or less similar effect. In was recently proposed to use riblets to guide the flow into oscillatory motion by changing the shape of riblets from conventional straight rods into sinusoidal rods.[17] By combining these two drag reduction mechanisms (riblets and oscillatory flow motion), it is hoped that the benefits of the two methods will also be combined.

*Postdoctoral Researcher, Institut Jean le Rond d'Alembert, AIAA Member, E-mail: peet@ccr.jussieu.fr

†Professor, Institut Jean le Rond d'Alembert

‡Research Engineer

This paper documents Large Eddy Simulation (LES) study of turbulent flow in a channel, one wall of which is covered with riblets of triangular cross-section, and the other wall is flat. Computations of three geometries are performed: conventional straight riblets (with the results compared to DNS data of Choi et al.[6]) and two cases of sinusoidal riblets with different wavelengthes of riblet oscillations. It is found that the wavelength of riblet oscillations equal to $3.22\,\delta$ results in a smaller drag reduction than the straight riblet case. However, if the wavelength is increased to $6\,\delta$, drag reduction achieved with the sinusoidal riblets is about 50% larger than that with the straight riblets, demonstrating clear benefits of the former method. Strong dependence of drag reduction properties on the oscillation period was also reported for the case of spanwise-oscillating wall,[10,18] phenomenon not yet understood.

II. Numerical Method and Simulation Parameters

LES code used in the present study is unstructured second-order incompressible solver with finite-volume scheme, Code_Saturne, developed at Électricité de France(EDF).[19] In addition to extensive testing of Code_Saturne performed in EDF,[19] LES of turbulent plane channel flow at $Re_\tau = 180$ was performed with this code as a part of the current study, and resulting turbulent mean flow and second-order quantities agree well with available DNS data.[17]

Computational geometry for riblet calculations consists of a channel whose top wall is a flat wall and bottom wall is covered with riblets. Riblets have triangular cross-section with the riblet ridge angle $\alpha = 60°$. The difference between straight riblets and sinusoidal riblets is highlighted in Figure 1. Sinusoidal riblet geometry has two more important parameters compared to straight riblets: amplitude a and wavelength λ of the oscillations. Parameters of the computational domain are summarized for the three simulated cases in Table 1 in δ units and in Table 2 in wall units. Here δ is half of the distance between the midpoint between tip and valley on a riblet wall and a flat wall and thus corresponds to the half-width of the plane channel with the same cross-sectional area. L_x and L_z are streamwise and spanwise computational periods (as periodic boundary conditions are used in these directions), s is the riblet spacing and h is the riblet height. For the two sinusoidal cases, wavelength λ and amplitude a are varied in a manner so that the maximum slope of the sinusoidal curve $2\,\pi\,a/\lambda$ remains constant corresponding to an angle $\beta = 11.3°$ (Figure 1(b)). Size of the computational domain is chosen large enough to guarantee that natural coherence of organized turbulence structures in a boundary layer is not disturbed by insufficient domain size ($L_x^+ > 300, L_z^+ > 100$).[20] Reynolds number based on δ and bulk velocity is 2730. This Reynolds number corresponds to $Re_\tau = 180$ based on a friction velocity which would develop in a plane channel flow with the same bulk Reynolds number. Computations are initialized by adding synthetic turbulent fluctuations to the laminar solution. Calculations are advanced with the time step $\Delta\,tU_b/\delta \sim 0.03$, or $\Delta\,t^+ \sim 0.3$.

Case	L_x/δ	L_z/δ	s/δ	h/δ	a/δ	λ/δ	$N_x \times N_y \times N_z$
Straight	3.22	0.93	0.1164	0.1	0	0	$16 \times 64 \times 128$
Sinus 1	3.22	0.93	0.1164	0.1	0.1	3.22	$16 \times 64 \times 128$
Sinus 2	6	0.93	0.1164	0.1	0.19	6	$32 \times 64 \times 128$

Table 1. Parameters of the computational domain in δ units.

Case	L_x^+	L_z^+	s^+	h^+	a^+	λ^+	$\Delta x^+ \times \Delta y^+ \times \Delta z^+$
Straight	580	165	21	18	0	0	$36 \times (0.4 - 14) \times 1.28$
Sinus 1	580	165	21	18	18	580	$36 \times (0.4 - 14) \times 1.28$
Sinus 2	1080	165	21	18	34	1080	$33 \times (0.4 - 14) \times 1.28$

Table 2. Parameters of the computational domain in wall units.

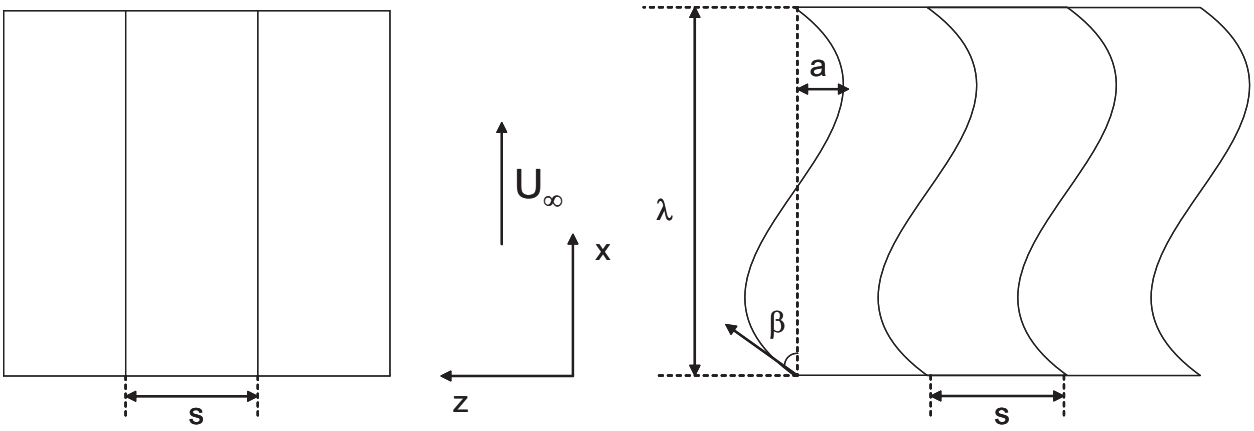

(a) Straight riblets

(b) Sinusoidal riblets

Figure 1. Comparison between straight and sinusoidal riblets. View of the riblet-covered surface from above.

III. Straight Riblets

In this section, results obtained by the LES simulations of straight riblets are shown. Three subgrid-scale models are investigated: classical Smagorinsky model[21] with van Driest wall functions,[22] modified Smagorinsky model[23] and dynamic Smagorinsky model[24] with local averaging. In a classical Smagorinsky model, eddy viscosity $\nu_{t,\,smag}$ is approximated as

$$\nu_{t,\,smag} = C_{smag}^2\,\Delta^2\,(2\,\overline{S}_{i\,j}\,\overline{S}_{i\,j}), \tag{1}$$

where Δ is the LES-filter width and $\overline{S}_{i\,j} = (\partial\,\overline{u}_i/\partial\,x_j + \partial\,\overline{u}_j/\partial\,x_i)/2$ is the filtered rate of strain tensor. C_{smag} is the Smagorinsky coefficient which, when van Driest wall functions are used, is defined as

$$C_{smag} = C_{0,\,smag}\,(1 - e^{-y^+/A}), \tag{2}$$

where $C_{0,\,smag}$ is the base constant chosen to be 0.0165 in the present second-order solver to minimize the dissipation, $A = 26$ is the van Driest constant and y^+ is the distance to the wall in wall units.

In a modified Smagorinsky model, eddy viscosity $\nu_{t,\,mod}$ is obtained as

$$\nu_{t,\,mod} = (\nu_{t,\,smag}^2 + \nu^2)^{1/2} - \nu, \tag{3}$$

where $\nu_{t,\,smag}$ is the eddy viscosity of a classical Smagorinsky model defined by equation (1) with C_{smag} defined by equation (2), ν is the laminar viscosity. This modification accounts for the dependence of ν_t on Δ/η, where η is the Kolmogorov scale, missing in a classical Smaroginsky model with constant coefficient.[23]

Results are compared with DNS calculations of Choi et al.[6] performed for the same geometry and a similar Reynolds number $Re_b = 2800$. The value of the accumulated time-averaged drag reduction R_D obtained with the three models versus the non-dimensional computational time tU_b/δ is presented in Figure 2(a). Drag reduction is defined as

$$R_D = \frac{D_f - D_r}{D_f} \times 100\%, \tag{4}$$

where

$$\begin{aligned} D_f &= \mu \int_{A_f} \frac{\partial\,u}{\partial\,n}\,d\,A_f, \\ D_r &= \mu \int_{A_r} \frac{\partial\,u}{\partial\,n}\,d\,A_r; \end{aligned} \tag{5}$$

D_f, D_r, A_f and A_r are the values of drag and the surface area for the flat and riblet walls, respectively. First, it is seen that quite a long time, tU_b/δ 1000, is required to reduce the fluctuations in R_D to about $\pm 0.5\%$. Classical Smagorinsky model and modified Smagorinsky model converge to R_D value of about $5.4 \pm 0.5\%$ at tU_b/δ 1000. Dynamic model with local averaging was run for a shorter time, so its computed

R_D value of 6.5%[17] would most likely drop down to $\sim$ 5.4% as well. This value is consistent with the typical drag reduction values for the riblets with triangular cross-section reported in other experimental and computational studies.[1–8] Drag reduction of 6% was obtained in DNS calculations of Choi et al.[6] However, their averaging time was only $tU_b/\delta \sim 330$, after which, according to their estimation, the remaining fluctuations of averaged wall-shear rates were about $\pm 2\%$. It is confirmed by the Figure 2(a) that fluctuations are still quite significant after the averaging time of $tU_b/\delta \sim 330$, indeed about $\pm 2\%$.

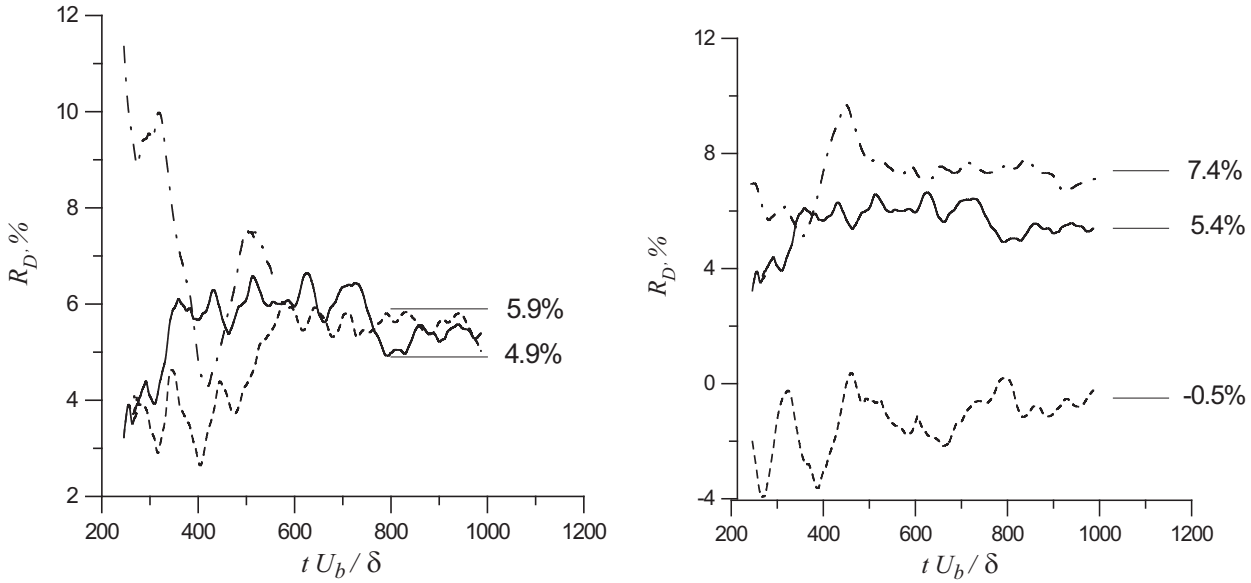

(a) Straight riblets. ———, classical Smagorinsky model; – – – modified Smagorinsky model; – · – · –, dynamic model with local averaging.

(b) Sinusoidal riblets. ———, straight case; – – – Sinus 1 case, $\lambda/\delta = 3.22$; – · – · –, Sinus 2 case, $\lambda/\delta = 6$.

Figure 2. Value of the drag reduction versus non-dimensional computational time.

Turbulence statistics for the three models is compared in Figure 3, where mean streamwise velocity as well as root-mean square velocity fluctuations are shown. Results from DNS of Choi et al.[6] are also plotted for comparison. Mean velocity is normalized with U_l to be consistent with the plots of Choi et al.[6] (U_l is the centerline velocity which would occur in a laminar plane channel flow with the same bulk velocity, i.e. $U_l = 1.5\,U_b$). Velocity fluctuations are normalized with U_c, where U_c is the turbulent centerline velocity. It can be seen that dynamic model with local averaging significantly underpredicts normal and spanwise Reynolds stresses. Misbehavior of the dynamic model is explained by the absence of averaging along the homogeneous directions as usually done for a plane channel.[17] Both classical Smagorinsky and modified Smagorinsky models show generally good agreement with DNS data,[6] but modified Smagorinsky model results in slightly higher values of normal and spanwise velocity fluctuations on a flat wall. Since superiority of the modified Smagorinsky model over the classical model was not observed in this case, the authors decided to choose classical Smagorinsky model for the calculations of sinusoidal riblets.

Drag reduction mechanism with the straight riblets as deduced from the current LES was highlighted in Ref. 17. It was confirmed by looking at snapshots of streamwise vorticity and three-dimensional coherent structures that quasi-streamwise vortices are displaced by the riblets away from the wall. Thus the surface area subjected to the downwash of high-speed fluid by the vortices is reduced leading to the subsequent decrease in drag.[6]

IV. Sinusoidal Riblets

Sinusoidal spanwise variation of the riblet shape is proposed in order to introduce an oscillating spanwise component into the near-wall mean flow. The hope is that such a flow will resemble the flow over spanwise-oscillating plate, for which significant drag reduction is known to occur compared to a stationary plate.[10–15] As laminar analysis shows,[17] resulting riblet crossflow boundary layer indeed closely resembles a Stokes layer which is a theoretical laminar solution for the flow over an oscillating wall.[25] Spanwise velocity profiles taken

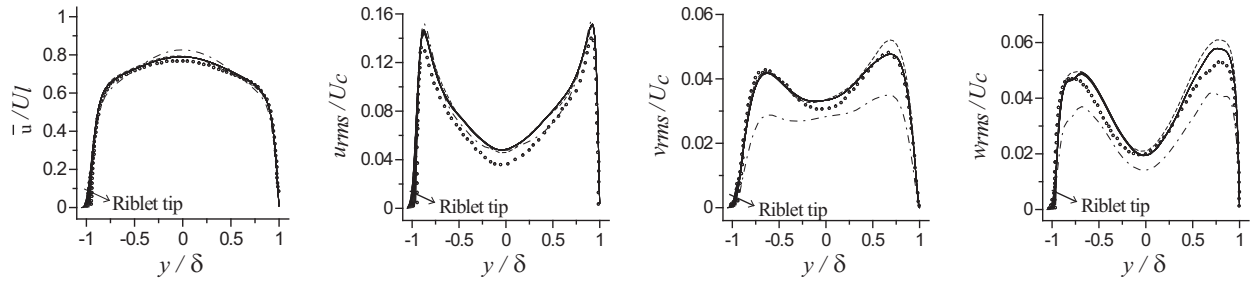

(a) Mean velocity. (b) u_{rms} (c) v_{rms} (d) w_{rms}

Figure 3. Turbulence statistics. ———, classical Smagorinsky model; – – – modified Smagorinsky model; – · – · –, dynamic model with local averaging, ○, DNS of Choi et al.

over different streamwise locations in a riblet boundary layer perfectly collapse when appropriate scaling is used with spanwise velocity profiles of a Stokes layer taken at the oscillation phase when the wall velocity is zero.[17]

In order to check whether this similarity of a riblet crossflow boundary layer with a Stokes layer over a spanwise-oscillating plate will further result in drag reduction benefits in a turbulent case, values of R_D defined in Equation (4) are plotted versus non-dimensional computational time in Figure 2(b) for cases 1 and 2 of sinusoidal riblets (see Tables 1 and 2) compared to a straight riblet case. It is seen that drag reduction is reduced to a negative value for the Sinus 1 case, where the wavelength of the oscillations is chosen to be $\lambda/\delta = 3.22$. When the oscillation wavelength is almost doubled to $\lambda/\delta = 6$, the drag reduction value rises to $7.4 \pm 0.5\%$, which is almost 50% larger than the drag reduction observed with the straight riblets. It is an author's belief that with the careful choice of riblet oscillation parameters it is possible to raise this value even higher.

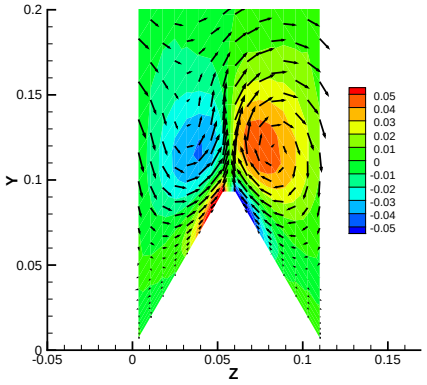

Figure 4. Mean streamwise vorticity, $\overline{\omega_x}\,\delta/U_l$, and mean velocity vectors $(\overline{v}, \overline{w})$ in the transverse plane for straight riblets.

To highlight the differences in the flow developed over straight and sinusoidal riblets, we look at the mean streamwise vorticity, $\overline{\omega_x}\,\delta/U_l$, and mean velocity vectors $(\overline{v}, \overline{w})$ in transverse planes. Figure 4 shows the transverse flow for the straight case, and Figure 5 - for two sinusoidal cases at three transverse planes, $x/\lambda = 0$, $x/\lambda = 1/4$ and $x/\lambda = 1/2$. For the straight riblets, a secondary flow is developed due to the turbulent momentum transfer from the central region to the riblet valley, and then away from the riblet valley to the riblet tip along the riblet surface.[6] For the sinusoidal riblets, a transverse motion is due to the turning of mean flow near the wall to follow a sinusoidal riblet shape. At $x/\lambda = 0$, the flow is turning in a positive spanwise direction, resulting in a positive streamwise vorticity on the surface; at $x/\lambda = 1/4$, the flow is aligned in the streamwise direction, and surface streamwise vorticity is largely diminished; at $x/\lambda = 1/2$, the flow has reversed to follow a negative spanwise direction, and large negative streamwise vorticity can now be seen at the surface. It is worth noting that maximum mean vorticity levels for sinusoidal cases, 0.3, are six times larger than corresponding mean vorticity levels of 0.05 in a straight case. Crossflow velocities and mean streamwise vorticity levels are similar for the two sinusoidal cases, consistent with the fact that an angle β determining an amplitude of spanwise velocity oscillations due to turning is the same for the two cases.

Instantaneous features of the flow above the riblet surfaces can be seen in Figure 6, where instantaneous streamwise vorticity, $\omega_x\,\delta/U_l$, and instantaneous velocity vectors (v, w) are plotted in a transverse plane for both straight and sinusoidal (Sinus 1 case) riblets. It is well known that for the straight riblet case coherent streamwise vortices formed in a turbulent boundary layer are displaced by the riblets away from the surface.[6,16] Coherent streamwise vortices usually come in pairs, co-rotating vortex alongside with the counter-rotating vortex, and are placed between the low-speed streaks, pumping high-speed fluid towards the surface, and low-speed fluid away from the surface. Existence of these coherent vortices is perfectly visible

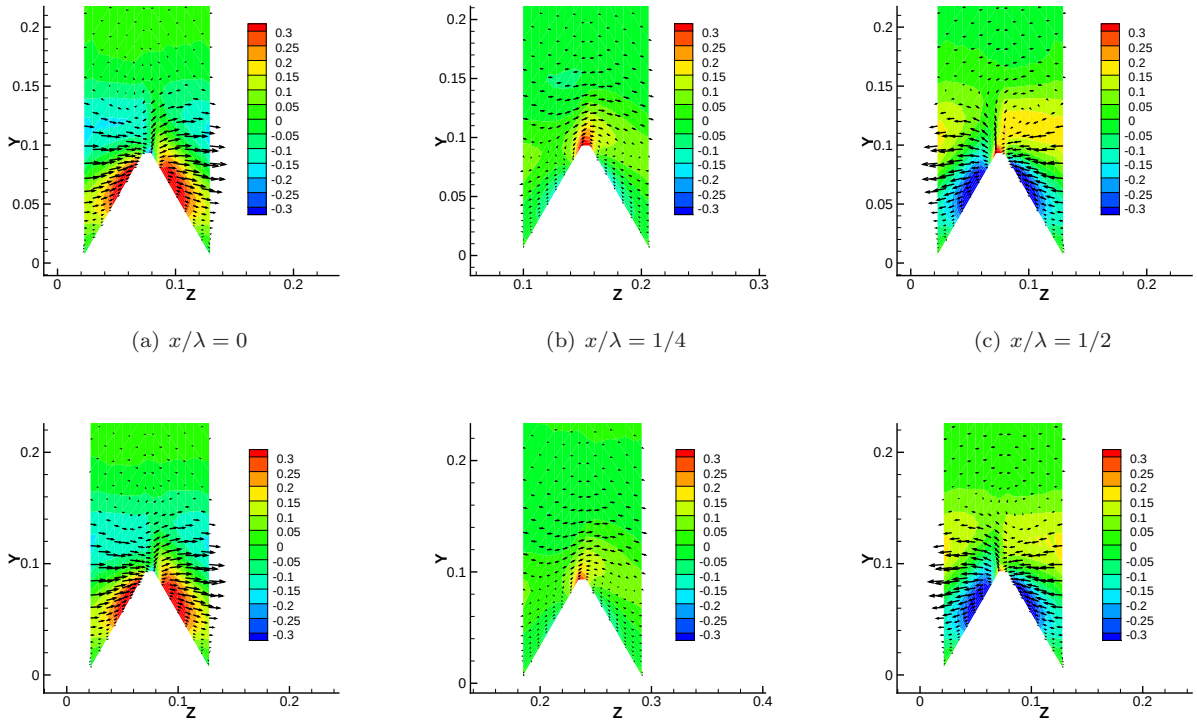

(a) $x/\lambda = 0$ (b) $x/\lambda = 1/4$ (c) $x/\lambda = 1/2$

(d) $x/\lambda = 0$ (e) $x/\lambda = 1/4$ (f) $x/\lambda = 1/2$

Figure 5. Mean streamwise vorticity, $\overline{\omega_x}\,\delta/U_l$, and mean velocity vectors $(\overline{v}, \overline{w})$ at three transverse planes for sinusoidal riblets. (a) – (c), $\lambda/\delta = 3.22$; (d)–(f), $\lambda/\delta = 6$.

in Figure 6(a). However, for sinusoidal riblets the structure of the turbulent boundary layer seems to be completely different. Co- and counter- rotating vortices are observed not alongside, but on top of each other. They are elongated in spanwise direction and flattened in vertical direction, and seem to be less chaotic. It looks like that vorticity formed on the riblet surface due to the turning of the flow is shed into the boundary layer and lifted above the surface by the crossflow motion, while it is convected downstream with the mean flow. A layer of vorticity of the opposite sign, shed from a point located half a wavelength downstream, is formed underneath it, and so on. Existence of four layers is observed, vorticity does not rise above the fourth layer due to the weakening of transverse crossflow motion with the distance from the wall. Such an organized vortex shedding inhibits the formation of irregular "classical" streamwise vortices and violates their spatial coherence, resulting in a reduction of turbulent near-wall burst activity and reduction of the turbulent contribution into a skin friction drag.[26] Further understanding of coherent vortical structures in a riblet surface boundary layer can be gained by looking at iso-surfaces of instantaneous streamwise vorticity, plotted in Figure 7. It is seen that the structures formed in a sinusoidal riblet boundary layer are thinner, longer, have a sinusoidal shape and, indeed, appear to be more organized than "classical" boundary layer structures.

Turbulence statistics for the two sinusoidal cases compared to the straight case is shown in Figure 8. Streamwise turbulence intensity is slightly increased for both sinusoidal cases compared to the straight case, probably due to the enhancement of fluctuations in u velocity caused by mean flow inhomogeneity in streamwise direction. However, crossflow turbulence, characterized by v_{rms} and w_{rms}, is significantly reduced for the two sinusoidal cases, consistent with the suppression in formation of irregular coherent streamwise vortices, observed in Figure 7(b). It is the crossflow turbulence which influences the skin friction drag. When transverse turbulent fluctuations are reduced, turbulent momentum transfer close to the surface is also reduced, and, consequently the shear stress is decreased.[8] Note that the turbulence statistics is changed not only on the riblet surface, but also on the flat surface, sine the presence of sinusoidal flow motion next to the bottom wall affects also the top wall in a low Reynolds number flow, such as in current simulations.

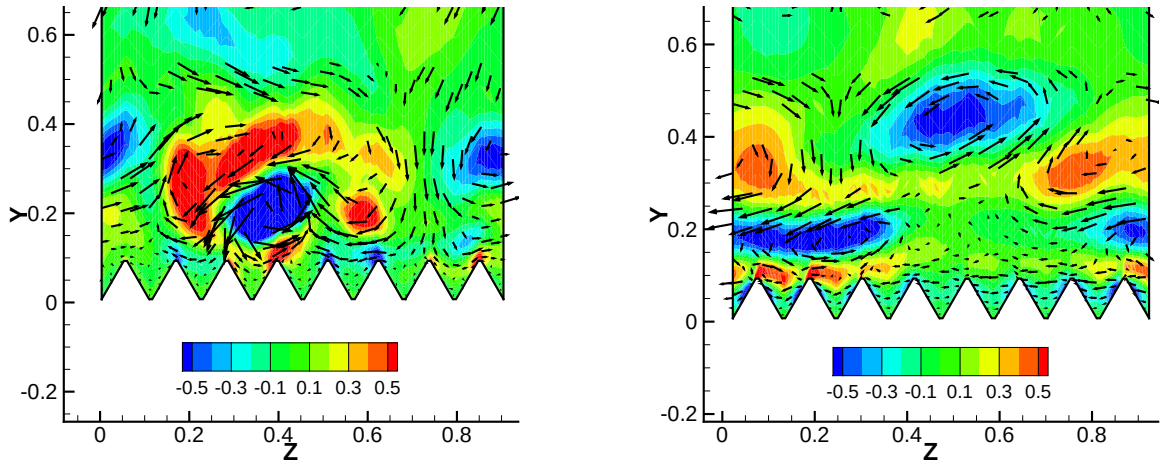

(a) Straight riblets (b) Sinusoidal riblets (Sinus 1 case)

Figure 6. Instantaneous streamwise vorticity, $\omega_x\,\delta/U_l$, and instantaneous velocity vectors (v, w) in a transverse plane.

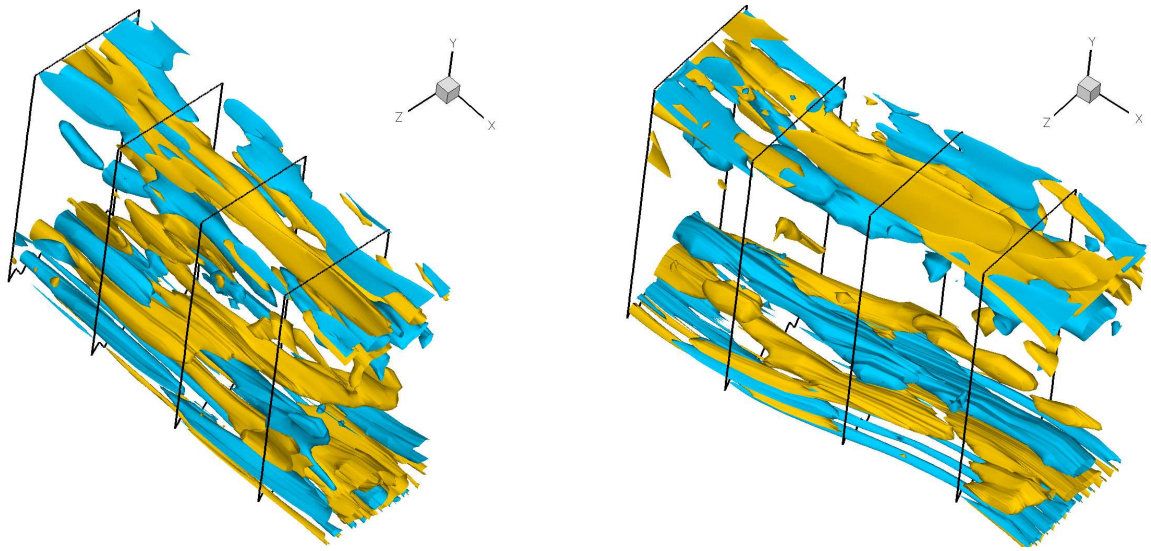

(a) Straight riblets (b) Sinusoidal riblets (Sinus 1 case)

Figure 7. Isosurfaces of instantaneous streamwise vorticity.

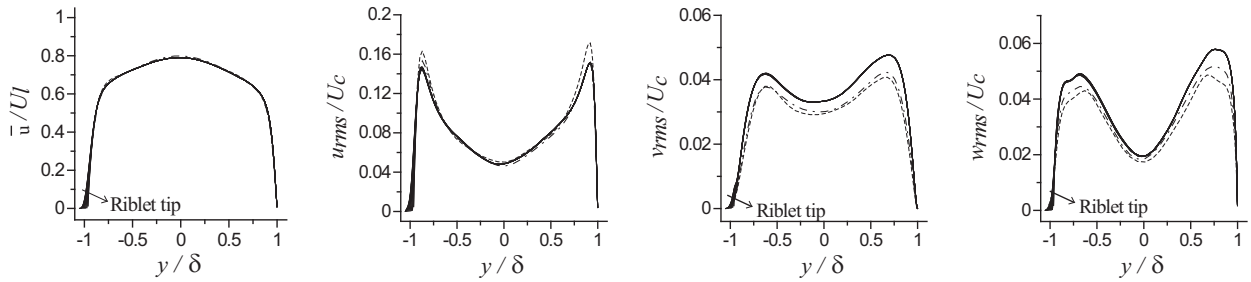

(a) Mean velocity. (b) u_{rms}/U_c (c) v_{rms}/U_c (d) w_{rms}/U_c

Figure 8. Turbulence statistics. ———, straight riblets; – – –, Sinus 1 case, $\lambda/\delta = 3.22$; – · – · –, Sinus 2 case, $\lambda/\delta = 6$.

V. Conclusions

It is shown in this paper that introducing spanwise sinusoidal variation to the riblet shape can be an effective drag reduction method showing benefits compared to the conventional straight riblets with the correct choice of geometrical parameters. Large Eddy Simulations are performed for the straight riblets and two sinusoidal riblets with different oscillation wavelengthes. Several turbulence models are considered for the straight riblet case and results are compared to DNS data[6] for the same configuration. Classical Smagorinsky model provides the best results for this case and is used for sinusoidal riblet calculations. For sinusoidal riblets, drag reduction depends strongly on the wavelength of the sinusoidal oscillations. For a smaller wavelength, $\lambda/\delta = 3.22$, no drag reduction is observed. For a larger value, $\lambda/\delta = 6$, drag reduction of 7.4% is achieved compared to 5.4% in a straight case. This signifies almost 50% of the drag reduction increase and it is believed that even higher benefits can be obtained by careful optimization of spanwise riblet variation parameters. Crossflow motion in transverse planes is very different for the straight and sinusoidal riblets, where it is dominated in the latter case by turning of the near-wall flow to follow the riblet shape. Consequently, the properties of coherent near-wall turbulent structures are also significantly modified. Turbulence statistics shows enhancement of streamwise fluctuations, and reduction of vertical and spanwise fluctuations for the case of sinusoidal riblets as compared to straight riblets. Reduction of crosslfow turbulence intensity is responsible for the reduction of turbulent contribution into the skin friction drag.

VI. Acknowledgements

This work is supported by Agence Nationale pour la Recherche (project PAN-H/READY).

References

[1]Walsh, M. J., "Drag Characteristics of V-Groove and Transverse Curvature Riblets," *Viscous Flow Drag Reduction*, ed. G. R. Hough, AIAA, New York, 1980, pp. 168–184.

[2]Walsh, M. J., "Turbulent Boundary Layer Drag Reduction Using Riblets," AIAA Paper 82–0169, 1982, New York.

[3]Walsh, M. J., "Riblets as a Viscous Drag Reduction Technique," *AIAA J.*, Vol. 21, 1983, pp. 485–486.

[4]Walsh, M. J. and Lindemann, A. M., "Optimization and Application of Riblets for Turbulent Drag Reduction," AIAA Paper 84–0347, 1984, New York.

[5]Walsh, M. J., "Riblets," *Viscous Drag Reduction in Boundary Layers*, eds. D. M. Bushnell and J. N. Heffner, AIAA, Washington, D.C., 1990, pp. 203–261.

[6]Choi, H., Moin, P., and Kim, J., "Direct Numerical Simulation of Turbulent Flow over Riblets," *J. Fluid Mech.*, Vol. 255, 1993, pp. 503–539.

[7]Goldstein, D., Handler, R., and Sirovich, L., "Direct Numerical Simulation of Turbulent Flow over Modelled Riblet Covered Surface," *J. Fluid Mech.*, Vol. 302, 1995, pp. 333–376.

[8]Bechert, D. W., Bruse, M., Hage, W., Hoeven, J. G. T. V. D., and Hoppe, G., "Experiments on Drag-Reducing Surfaces and Their Optimization with an Adjustable Geometry," *J. Fluid Mech.*, Vol. 338, 1997, pp. 59–87.

[9]Gad-El-Hak, M., *Flow Control*, Cambridge University Press, 2000.

[10]Jung, W. J., Mangiavacchi, N., and Akhavan, R., "Suppression of Turbulence in Wall Bounded Flows by High-Frequency Spanwise Oscillations," *Phys. Fluids*, Vol. 8, 1992, pp. 1605–1607.

[11]Laadhari, F., Skandaji, L., and Morel, R., "Turbulence Reduction in a Boundary Layer by a Local Spanwise Oscillating Surface," *Phys. Fluids*, , No. 10, 1994, pp. 3218–3220.

[12]Choi, K.-S. and Graham, M., "Drag Reduction of Turbulent Pipe Flows by Circular-Wall Oscillation," *Phys. Fluids*, Vol. 10, No. 1, 1998, pp. 7–9.

[13]Choi, K.-S., DeBisschop, J. R., and Clayton, B. R., "Turbulent Boundary-Layer Control by Means of Spanwise-Wall Oscillation," *AIAA J.*, Vol. 36, 1998, pp. 1157.

[14]Choi, K.-S. and Clayton, B. R., "The Mechanism of Turbulent Drag Reduction with Wall Oscillation," *Int. J. Heat and Fluid Flow*, Vol. 22, 2001, pp. 1–9.

[15]Choi, K.-S., "Near-Wall Structure of Turbulent Boundary Layer with Spanwise-Wall Oscillation," *Phys. Fluids*, Vol. 14, No. 7, 2002, pp. 2530–2542.

[16]Choi, K.-S., "Near-Wall Structure of a Turbulent Boundary Layer with Riblets," *J. Fluid Mech.*, Vol. 208, 1989, pp. 417–458.

[17]Peet, Y., Sagaut, P., and Charron, Y., "Towards Large Eddy Simulations of Turbulent Drag Reduction Using Sinusoidal Riblets," WSEAS Paper 565-355, 2007, Presented at the 5th IASME/WSEAS International Conference on Fluid Mechanics and Aerodynamics, Vouliagmeni, Greece, August 25-27, 2007.

[18]Baron, A. and Quadrio, M., "Turbulent Boundary Layer Over Riblets: Conditional Analysis of Ejection-Like Events," *Int. J. Heat and Fluid Flow*, Vol. 18, 1997, pp. 188–196.

[19]Archambeau, F., Méchitoua, N., and Sakiz, M., "Code_Saturne: a Finite Volume Code for the Computation of Turbulent Incomressible Flows - Industrial Applications," *Int. J. Fin. Vol.*, Vol. 1, 2004.

[20]Jiménez, J. and Moin, P., "The Minimal Flow Unit in Near-Wall Turbulence," *J. Fluid Mech.*, Vol. 225, 1991, pp. 213–240.

[21]Smagorinsky, J., "General Circulation Experiments with the Primitive Equations," *Journal of Monthly Weather Review*, Vol. 91, No. 3, 1963, pp. 99–164.

[22]Driest, E. R. V., "Turbulent Boundary Layer in Compressible Fluids," *J. Aerospace Sci.*, Vol. 18, No. 3, 1951, pp. 145–160.

[23]Meyers, J. and Sagaut, P., "On the Model Coefficient for the Standard and the Variational Multi-Scale Smagorinsky Model," *J. Fluid Mech.*, Vol. 569, 2006, pp. 287–319.

[24]Germano, M., Piomelli, U., Moin, P., and Cabot, W. H., "A Dynamic Subgrid-scale Eddy Viscosity Model," *Physics of Fluids, A3*, 1991, pp. 1760–1765.

[25]Schlichting, H., *Boundary-layer theory*, Berlin; New York: Springer, 8th ed., 2000.

[26]Fukagata, K., Iwamoto, K., and Kasagi, N., "Contribution of Reynoolds stress distribution to the skin friction in wall-bounded flows," *Phys. Fluids.*, Vol. 14, 2002, pp. L73.